

Supporting Information

Tunnel Dependent Supercapacitance of MnO₂: Effects of Crystal Structure

Congting Sun, Yuanjian Zhang, Shuyan Song, Dongfeng Xue*

State Key Laboratory of Rare Earth Resource Utilization, Changchun Institute of Applied Chemistry, Chinese Academy of Sciences, 5625 Renmin Street, Changchun 130022, P. R. China

E-mail: dongfeng@ciac.jl.cn

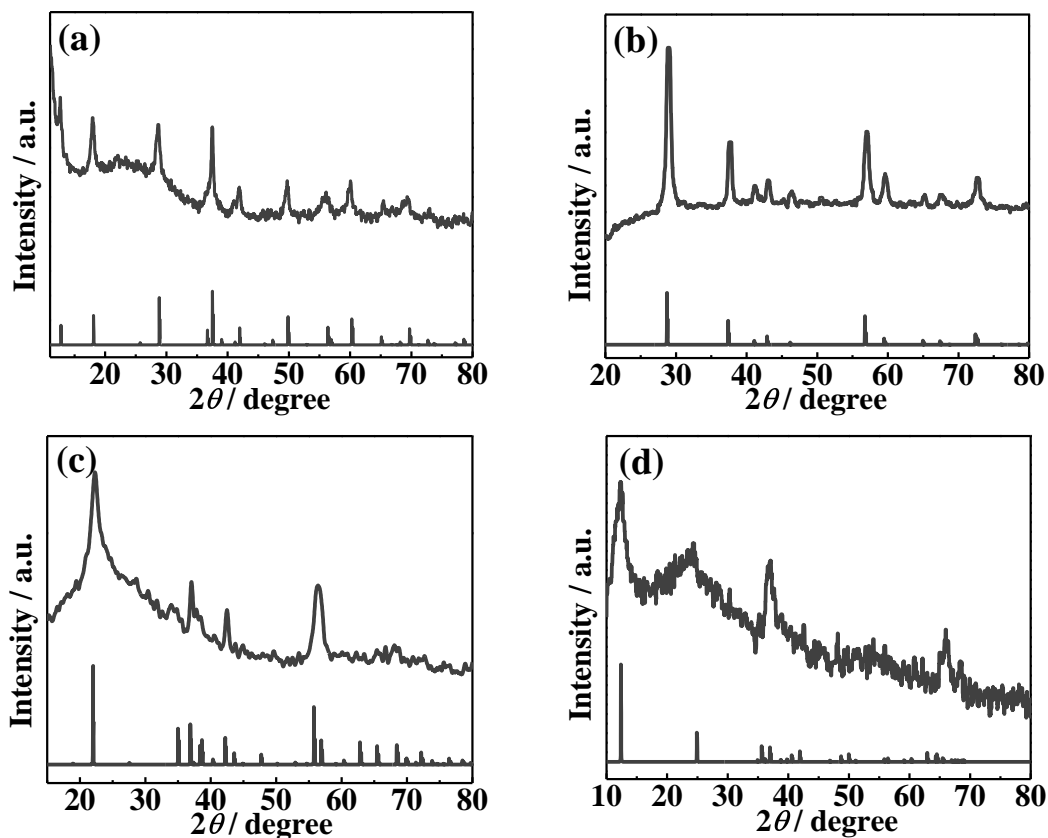


Figure S1. XRD patterns of the as-prepared a) α - , b) β - , c) γ - , and d) δ -MnO₂.

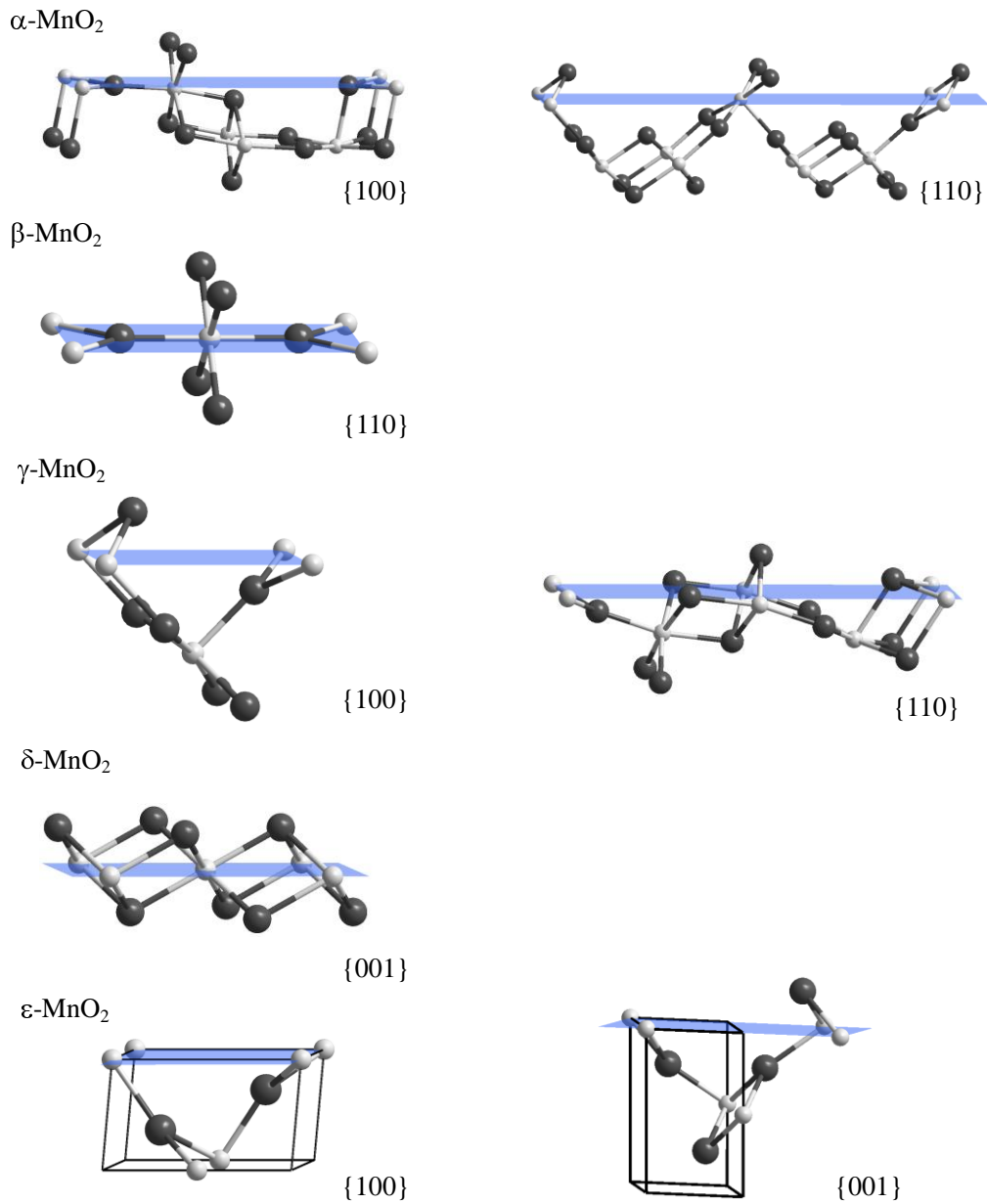


Figure S2. Exposed crystal surfaces of α -, β -, γ -, δ -, and $\varepsilon\text{-MnO}_2$.

Table S1. Density of Mn centers at (hkl) surfaces of MnO_2

| Crystal surface | N_{Mn} | $S (\text{nm}^2)$ | $\rho_{\text{Mn}} (\text{nm}^{-2})$ |
|------------------------------------|-----------------|-------------------|-------------------------------------|
| $\alpha\text{-MnO}_2 \{100\}$ | 4 | 0.28 | 14.28 |
| $\alpha\text{-MnO}_2 \{110\}$ | 6 | 0.40 | 15.18 |
| $\beta\text{-MnO}_2 \{110\}$ | 2 | 0.18 | 11.16 |
| $\gamma\text{-MnO}_2 \{100\}$ | 2 | 0.13 | 15.74 |
| $\gamma\text{-MnO}_2 \{110\}$ | 4 | 0.29 | 13.58 |
| $\delta\text{-MnO}_2 \{001\}$ | 2 | 0.15 | 13.56 |
| $\varepsilon\text{-MnO}_2 \{100\}$ | 2 | 0.12 | 16.27 |
| $\varepsilon\text{-MnO}_2 \{001\}$ | 1 | 0.07 | 14.88 |

Table S2. Summary of various reported MnO₂ electrode materials for supercapacitors

| Electrode materials | Electrolyte | C (mol L ⁻¹) | Current density (A g ⁻¹) / scan rate (mV s ⁻¹) | Mass loading (mg cm ⁻²) | Specific capacitance (F g ⁻¹) | SC/SC(α-MnO ₂) | Ref. |
|---------------------|---------------------------------|--------------------------|--|-------------------------------------|---|----------------------------|--------------------------------|
| α-MnO ₂ | Na ₂ SO ₄ | 0.1 | 1 A g ⁻¹ | 0.5 | 240 | 1.00 | Devaraj & Munichandraiah, 2008 |
| β-MnO ₂ | Na ₂ SO ₄ | 0.1 | 1 A g ⁻¹ | 0.5 | 9 | 0.04 | Devaraj & Munichandraiah, 2008 |
| γ-MnO ₂ | Na ₂ SO ₄ | 0.1 | 1 A g ⁻¹ | 0.5 | 107 | 0.45 | Devaraj & Munichandraiah, 2008 |
| δ-MnO ₂ | Na ₂ SO ₄ | 0.1 | 1 A g ⁻¹ | 0.5 | 236 | 0.98 | Devaraj & Munichandraiah, 2008 |
| α-MnO ₂ | Na ₂ SO ₄ | 0.1 | 1 A g ⁻¹ | 0.5 | 297 | 1 | Devaraj & Munichandraiah, 2008 |
| β-MnO ₂ | Na ₂ SO ₄ | 0.1 | 1 A g ⁻¹ | 0.5 | 9 | 0.03 | Devaraj & Munichandraiah, 2008 |
| γ-MnO ₂ | Na ₂ SO ₄ | 0.1 | 1 A g ⁻¹ | 0.5 | 107 | 0.36 | Devaraj & Munichandraiah, 2008 |
| δ-MnO ₂ | Na ₂ SO ₄ | 0.1 | 1 A g ⁻¹ | 0.5 | 236 | 0.79 | Devaraj & Munichandraiah, 2008 |
| α-MnO ₂ | K ₂ SO ₄ | 0.5 | 5 mV s ⁻¹ | 11 | 125 | 1.00 | Ghodbane <i>et al.</i> , 2009 |
| β-MnO ₂ | K ₂ SO ₄ | 0.5 | 5 mV s ⁻¹ | 11 | 28 | 0.22 | Ghodbane <i>et al.</i> , 2009 |
| γ-MnO ₂ | K ₂ SO ₄ | 0.5 | 5 mV s ⁻¹ | 11 | 87 | 0.70 | Ghodbane <i>et al.</i> , 2009 |
| δ-MnO ₂ | K ₂ SO ₄ | 0.5 | 5 mV s ⁻¹ | 11 | 225 | 1.80 | Ghodbane <i>et al.</i> , 2009 |
| α-MnO ₂ | K ₂ SO ₄ | 0.1 | 5 mV s ⁻¹ | 100 μm thick film | 150 | 1.00 | Brousse <i>et al.</i> , 2006 |
| β-MnO ₂ | K ₂ SO ₄ | 0.1 | 5 mV s ⁻¹ | 100 μm thick film | 5 | 0.03 | Brousse <i>et al.</i> , 2006 |
| γ-MnO ₂ | K ₂ SO ₄ | 0.1 | 5 mV s ⁻¹ | 100 μm thick film | 30 | 0.20 | Brousse <i>et al.</i> , 2006 |
| δ-MnO ₂ | K ₂ SO ₄ | 0.1 | 5 mV s ⁻¹ | 100 μm thick film | 80 | 0.53 | Brousse <i>et al.</i> , 2006 |
| α-MnO ₂ | Na ₂ SO ₄ | 0.5 | 0.5 A g ⁻¹ | — | 87 | 1.00 | Cui <i>et al.</i> , 2011 |
| γ-MnO ₂ | Na ₂ SO ₄ | 0.5 | 0.5 A g ⁻¹ | — | 37 | 0.43 | Cui <i>et al.</i> , 2011 |
| δ-MnO ₂ | Na ₂ SO ₄ | 0.5 | 0.5 A g ⁻¹ | — | 143 | 1.64 | Cui <i>et al.</i> , 2011 |

In general, the specific capacitance of MnO_2 decreases with increasing thickness of the electrode layer (or film) due to the low electronic and ionic conductivities of MnO_2 . In order to exclude such influence factor, we selected the experimental data with the identical electrochemical tests for α -, β -, γ -, and δ - MnO_2 from previous reports (Devaraj & Munichandraiah, 2008; Ghodbane *et al.*, 2009; Brousse *et al.*, 2006; Cui *et al.*, 2011).

Different crystal sizes can lead to the variation of effective Mn centers for Faradaic reaction, consequently varying the specific capacitance of MnO_2 . According to the relationship of $SC \propto X_{\text{Mn}}^{\text{effective}}$, the range of the ratio of $SC(\text{MnO}_2)/SC(\alpha\text{-MnO}_2)$ can be deduced, the extreme values are given as

$$[SC(\text{MnO}_2)/SC(\alpha\text{-MnO}_2)]_{\min} = [SC(\text{MnO}_2)]_{\min}/[SC(\alpha\text{-MnO}_2)]_{\max} \quad (\text{S1})$$

$$[SC(\text{MnO}_2)/SC(\alpha\text{-MnO}_2)]_{\max} = [SC(\text{MnO}_2)]_{\max}/[SC(\alpha\text{-MnO}_2)]_{\min} \quad (\text{S2})$$

By combining with Equation (4), Equations (S1) and (S2) become

$$[SC(\text{MnO}_2)/SC(\alpha\text{-MnO}_2)]_{\min} = [X_{\text{Mn}}^{\text{effective}}(\text{MnO}_2)]_{\min}/[X_{\text{Mn}}^{\text{effective}}(\alpha\text{-MnO}_2)]_{\max} \quad (\text{S3})$$

$$[SC(\text{MnO}_2)/SC(\alpha\text{-MnO}_2)]_{\max} = [X_{\text{Mn}}^{\text{effective}}(\text{MnO}_2)]_{\max}/[X_{\text{Mn}}^{\text{effective}}(\alpha\text{-MnO}_2)]_{\min} \quad (\text{S4})$$

As shown in Figure S3, it can be found that the ratios of $SC(\text{MnO}_2)/SC(\alpha\text{-MnO}_2)$ in previous experimental measurements are included within the calculated ranges, validating our present calculations.

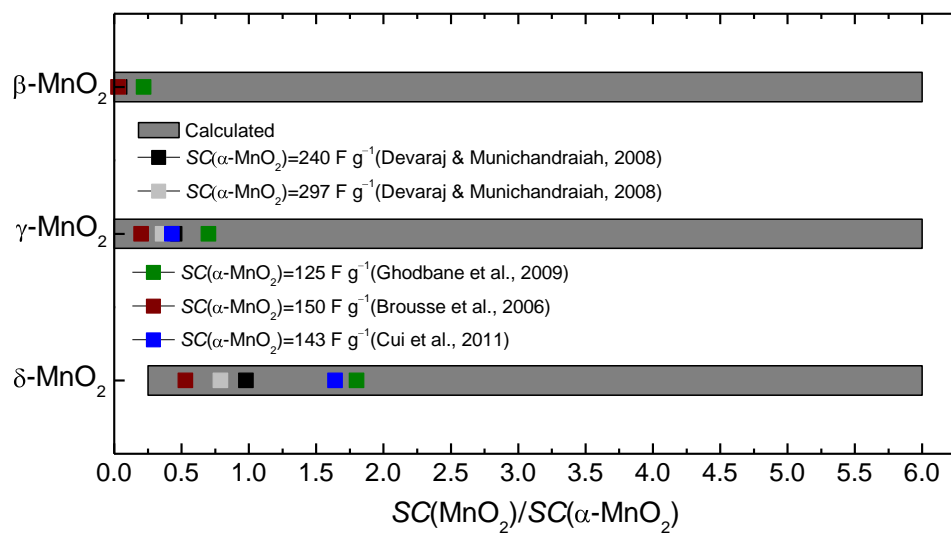


Figure S3. Comparison of calculted and experimental $SC(\text{MnO}_2)/SC(\alpha\text{-MnO}_2)$.

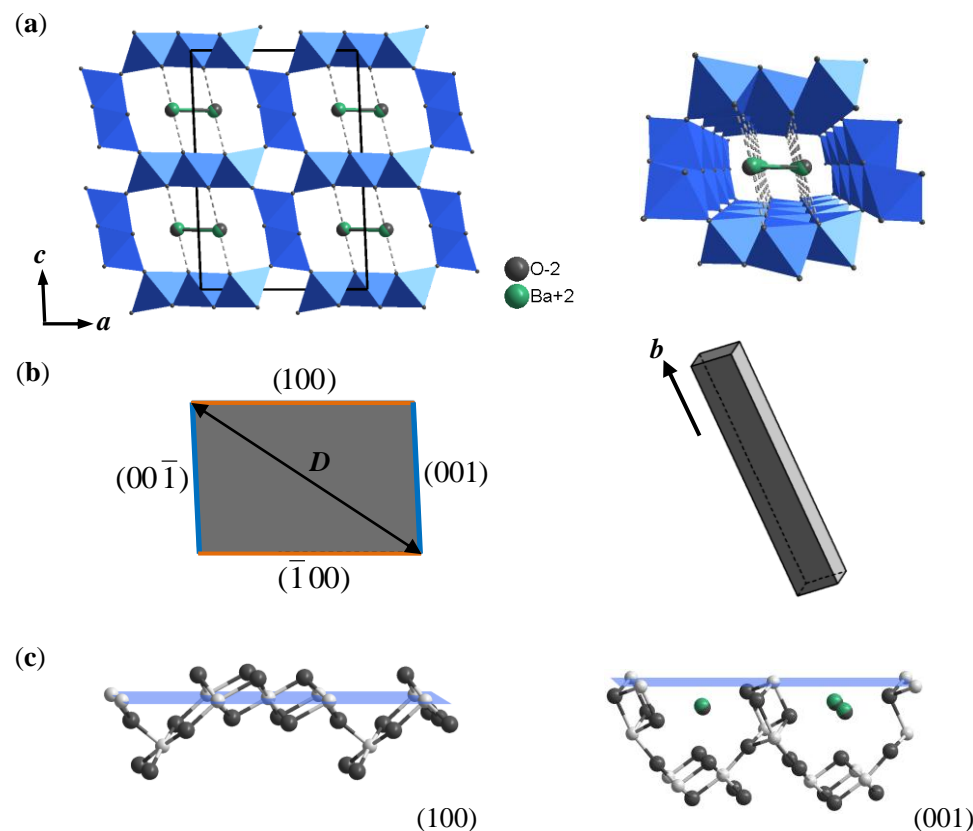


Figure S4. Crystallographic characteristics and growth behaviors of OMS-6 (2×3 tunnel).

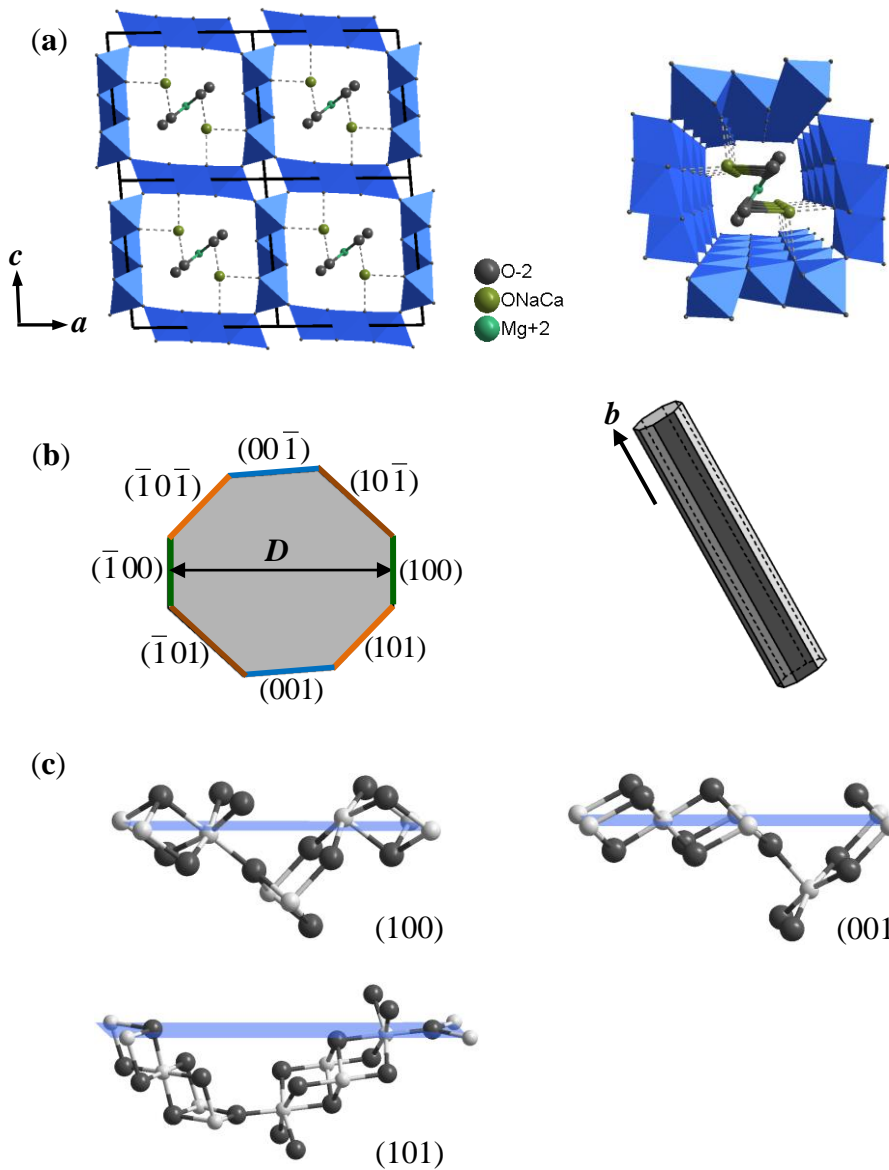


Figure S5. Crystallographic characteristics and growth behaviors of todorokite (3×3 tunnel).

References

- Brousse, T., Toupin, M., Dugas, R. Athouel, L., Crosnier, O. & Belanger, D. (2006). *J. Electrochem. Soc.* **153**, A2171– A2180.
- Cui, D., Gao, K., Lu, P., Yang, H., Liu, Y. & Xue, D. (2011). *Funct. Mater. Lett.* **4**, 57–60.
- Devaraj, S. & Munichandraiah, N. (2008). *J. Phys. Chem. C* **112**, 4406–4417.
- Ghodbane, O., Pascal, J.-L. & Favier, F. (2009). *ACS Appl. Mater. Inter.* **1**, 1130–1139.